Journal of Materials Chemistry B

Accepted Manuscript

This article can be cited before page numbers have been issued, to do this please use: H. Vilaça, G. Pereira, T. Castro, B. Hermenegildo, J. Shi, T. Q. Faria, N. Micaelo, R. Brito, B. Xu, E. M. S. Castanheira, J. A. Martins and P. M. Ferreira, *J. Mater. Chem. B*, 2015, DOI: 10.1039/C5TB00501A.

ROYAL SOCIETY OF CHEMISTRY

www.rsc.org/materialsB

View Article Online
DOI: 10.1039/C5TB00501A

Journal Name

RSCPublishing

ARTICLE

New self-assembled supramolecular hydrogels based on dehydropeptides

Cite this: DOI: 10.1039/xoxxooooox

Received ooth January 2012,
Accepted ooth January 2012

DOI: 10.1039/xoxxooooox

www.rsc.org/

H. Vilaça,[a] G. Pereira,[a] T. G. Castro,[a] B. F. Hermenegildo,[b] J. Shi,[c] T. Q. Faria,[d] N. Micaêlo,[a] R. M. M. Brito,[d] B. Xu,[c] E. M. S. Castanheira,[b] J. A. Martins,*[a] P. M. T. Ferreira*[a]

Supramolecular hydrogels rely on small molecules that self-assemble in water as a result of the cooperative effect of several relatively weak intermolecular interactions. Peptide-based low molecular weight hydrogelators have attracted enormous interest owing to the simplicity of small molecules combined with the versatility and biocompatibility of peptides. In this work, naproxen, a well known non-steroidal anti-inflammatory drug, was *N*-conjugated with various dehydrodipeptides to give aromatic peptide amphiphiles that resist proteolysis. Molecular dynamic simulations were used to obtain insight into the underlying molecular mechanism of self-assembly and to rationalize the design of this type of hydrogelators. The results obtained were in excellent agreement with the experimental observations. Only dehydrodipeptides having at least one aromatic amino acid gave hydrogels. The characterization of the hydrogels was carried out using transmission electron microscopy (TEM), circular dichroism (CD), fluorescence spectroscopy and also rheological assays.

Introduction

The preparation of biomaterials, such as hydrogels, using a "bottom-up" approach is based on molecular self-assembly through non-covalent interactions such as hydrogen bonding, Van der Waals forces and π-π and electrostatic interactions. Small peptides with bulky aromatic moieties can self-assemble into nanostructures that interweave giving three-dimensional (3D) networks that entrap water giving biocompatible and biodegradable hydrogels. These biomaterials have a wide range of applications, from drug delivery to tissue engineering and regenerative medicine.[1-8] One limitation of peptide based hydrogelators is their susceptibility to enzymatic hydrolysis, which shortens their *in vivo* lifetime and narrows the scope of their application. One of the strategies used to circumvent this limitation is to introduce non-proteinogenic amino acids into peptide hydrogelators.[9-13] Recently Xu *et al.* described the synthesis of new hydrogelators based on dipeptides containing unnatural *D*-amino acids *N*-capped with naproxen.[14] The *D*-amino acids in the conjugates not only increased the proteolytic stability of the hydrogelators but also enhanced their selectivity for inhibiting cyclooxygenase-2 (COX-2). The same authors also prepared and studied other peptides *N*-conjugated with other NSAID drugs, namely ibuprofen and flurbiprofen.[15]

In this work a multidisciplinary approach that combines molecular dynamic simulations with experimental results was devised for developing new efficient dehydropeptide hydrogelators. Five dehydrodipeptides *N*-conjugated with naproxen were prepared and studied. These compounds were designed taking into consideration several factors: dehydroamino acids[16-21] are known to increase the resistance of peptides against proteolytic enzymes, the naproxen-capped hydrogelators (and hydrogels) are likely to retain the NSAID properties of naproxen;[14,15] the naphthalene moiety of naproxen is prone to engage in intermolecular π-π stacking interactions as described for other peptide hydrogels functionalised with naphthalene moieties.[12,14,15,22]

The goal of this work was to understand the self-assembly behaviour of aromatic dehydrodipeptide amphiphiles and to create a rational basis for the design of new dehydropeptide hydrogelators. Molecular dynamic simulations, together with characterization assays [circular dichroism (CD), fluorescence spectroscopy, transmission electron microscopy (TEM) and rheometry], evidenced the propensity of dehydrodipeptides containing an aromatic amino acid and *N*-conjugated to a polyaromatic moiety to self-assemble into nanostructures that give hydrogels. Furthermore this new class of hydrogelators revealed to resist proteolytic degradation.

View Article Online
DOI: 10.1039/C5TB00501A
Journal Name

Results and discussion

Synthesis

Five new dehydrodipeptides *N*-protected with naproxen (Npx) were prepared from the corresponding methyl esters of *N*-*tert*-butoxycarbonyl-*β*-hydroxydipeptides. The strategy deployed involved a dehydration reaction followed by cleavage of the *tert*-butoxycarbonyl group (Boc), reaction with (*S*)-(+)-naproxen chloride and alkaline hydrolysis of the methyl esters (Scheme 1). The dehydroamino acids used were dehydrophenylalanine (ΔPhe) and dehydroaminobutyric acid (ΔAbu). This synthetic methodology was chosen to avoid racemization issues concerning the naproxen moiety. The *N*,*C*-diprotected dipeptides having a *β*-hydroxyamino acid (Scheme 1, **1a-e**) were dehydrated in good to high yields by treatment with *tert*-butyldicarbonate (Boc_2O) and 4-dimethylaminopyridine (DMAP) followed by *N*,*N*,*N'*,*N'*-tetramethylguanidine (TMG)[17] (Scheme 1, **2a-e**). The Boc group was removed with trifluoroacetic acid (TFA) (Scheme 1, **3a-e**) and the *N*-deprotected dehydrodipeptides were conjugated with (*S*)-(+)-naproxen (Scheme 1, **4a-e**). Finally, the methyl esters were removed by treatment with a solution of NaOH (1 M) affording compounds **5a-e** in good yields (Scheme 1).

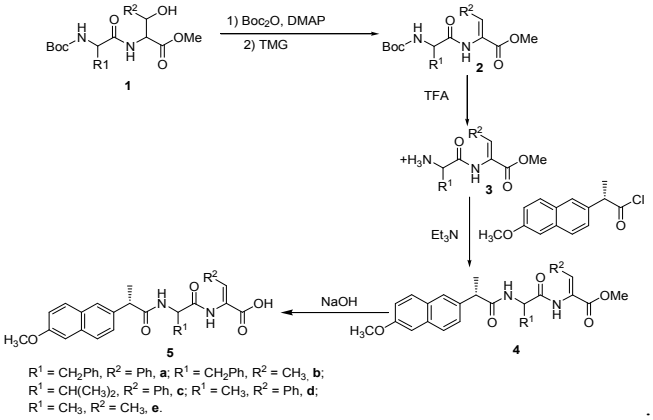

Scheme 1. Synthesis of dehydrodipeptides *N*-conjugated to naproxen (Npx): Npx-*L*-Phe-*Z*-ΔPhe-OH, **5a**; Npx-*L*-Phe-*Z*-ΔAbu-OH, **5b**; Npx-*L*-Val-*Z*-ΔPhe-OH, **5c**; Npx-*L*-Ala-*Z*-ΔPhe-OH, **5d**; Npx-*L*-Ala-*Z*-ΔAbu-OH, **5e**

The stereochemistry of compounds **2-5** was confirmed by Nuclear Overhauser (NOE) difference experiments by irradiating the α-NH proton of the dehydroamino acid residue and observing NOE enhancements in the signals of the *β*-methyl or *β*-phenyl protons. All ^{1}H NMR spectra of compounds **5a-e** in dimethylsulfoxide (DMSO-d_6) show one doblet and two singlets between 8.11 pm and 12.67 ppm due to the NH and CO_2H protons. The *β*-CH proton of the dehydroamino acid residues appears in the aromatic region in the case of dehydrophenylalanine and as a quartet near 6.5 ppm for dehydroaminobutyric acid. In the ^{13}C NMR spectra of these compounds the signals assigned to the *β*-carbon atoms of the dehydroamino acid residues appear in a narrow zone of high chemical shift between 131.81 ppm and 133.14 ppm. This is due to deprotection resulting from conjugation of the *α*,*β*-double bond with the carbonyl group.

Molecular Dynamic Simulations

Molecular dynamic simulations (MD) were carried out for all dehydrodipeptides prepared (**5a-e**) to examine the process spontaneous of self-assembly. The peptides were placed in cubic boxes of 4.5 x 4.5 x 4.5 mm solvated with the SPC water model.[23] The average number of clusters observed for each peptide is presented in Table 1. This analysis was carried out by calculating the number of peptides that are clustered using a cut-off of 1.4 nm for each simulation frame and averaged over the last 20 ns sampling time. The average number of intermolecular hydrogen bonds was calculated and averaged over the same time interval. The number of *π*-stacking interactions was divided by the number of peptides present in the simulation box and normalized by the number of simulated frames (last 20 ns). This average percentage of *π*-*π* interaction is read as the number of *π*-stacking / number of peptides in solution. Different types of *π*-stacking interactions were considered were: sandwich (S), parallel displaced (PD) or T-shaped (T). Experimental and theoretical data[24] were used to define the cut-off distances and angles between aromatic groups that characterize these types of *π*-stacking interactions. The intermolecular π-stacking interactions analyzed were those between naproxen groups, naproxen and the aromatic moieties of phenylalanine (Phe) and dehydrophenylalanine (ΔPhe) and between the phenyl groups of the two aromatic amino acid residues. All of these types of *π*-stacking interactions could be found solely for peptide **5a**, the other peptides show only some of these types of interactions. In the case of peptide **5e** the only π-stacking interactions observed are those between the naproxen moieties.

Journal Name

View Article Online
DOI: 10.1039/C5TB00501A ARTICLE

Table 1. Average number of clusters, hydrogen bonds and percentage of intra/intermolecular π-stacking interactions observed for each system. The total number of π-stacking interactions and also the individual contribution of each π-stacking geometry, S, PD and T, are shown. Standard deviation for the first two analyses is shown in parenthesis.

		Npx-Phe-ΔPhe-OH, **5a**	Npx-Phe-ΔAbu-OH, **5b**	Npx-Val-ΔPhe-OH, **5c**	Npx-Ala-ΔPhe-OH, **5d**	Npx-Ala-ΔAbu-OH, **5e**
Average number of clusters		3.2 (±0.10)	2.4 (±0.09)	2.8 (±0.08)	3.8 (±0.10)	4.5 (±0.09)
Average number of hydrogen bonds		3.8 (±0.04)	4.7 (±0.04)	3.5 (±0.04)	3.2 (±0.05)	3.7 (±0.04)
Percentage of π stacking interactions[a]	Npx-Npx	8.5 (S: 5.1; PD: 2.0; T: 1.4)	6.5 (S: 4.3; PD: 1.1; T: 1.1)	7.0 (S: 4.5; PD: 1.5; T: 1.0)	6.3 (S: 4.4; PD: 1.5; T: 0.4)	11.3 (S: 7.7; PD: 2.3; T: 1.3)
	Npx-Phe	3.6 (S: 1.9; PD: 0.7; T: 1.0)	4.5 (S: 2.5; PD: 1.1; T: 0.9)	—	—	—
	Npx-ΔPhe	1.7 (S: 0.8; PD: 0.4; T: 0.5)	—	2.7 (S: 1.3; PD: 0.5; T: 0.9)	2.0 (S: 0.9; PD: 0.4; T: 0.7)	—
	Phe-Phe	0.5 (S: 0.1; PD: 0.1; T: 0.3	0.6 (S: 0.2; PD: 0.1; T: 0.3)	—	—	—
	ΔPhe-ΔPhe	0.4 (S: 0.1; T: 0.3)	—	0.1 (T: 0.1)	0.2 (PD: 0.1; T: 0.1)	—
	Phe-ΔPhe	0.8 (S: 0.1; PD: 0.2; T: 0.5)	—	—	—	—
	Total	15.5	11.6	9.8	8.5	11.3

[a] Sandwich (S): $R \leq 4.5$ Å and $\theta \leq 15°$ or $\theta \geq 165°$; Parallel Displaced (PD): $R \leq 4.0$ Å and $15° < \theta < 30°$ or $150° < \theta < 165°$; T-shaped (T): $R \leq 3.5$ Å and $\theta \leq 10°$.

Figure 1 shows the clustering arrangement of a given frame taken from the simulation trajectory of **5a-e**.

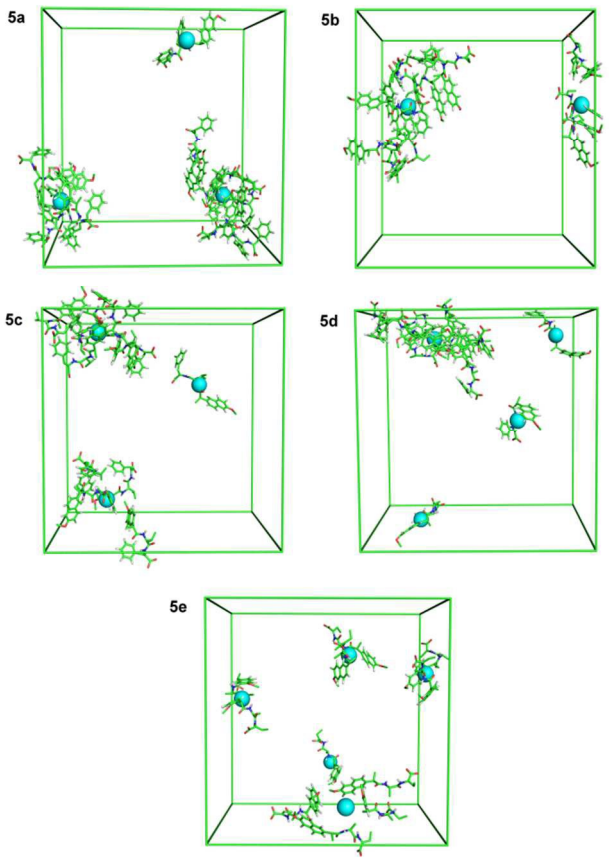

Figure 1. Snapshot of the MDS of peptides **5a-e** after equilibration. The water molecules have been omitted for better viewing of the peptides. The spheres in cyan represent the geometric center of each cluster. Figures were obtained with Pymol.[25]

Visual analysis of the clustering behaviour within each frame clearly shows self-aggregation of peptides **5a-d**, and, poor aggregation of peptide **5e**. Hydrogelators **5b** and **5c** show the lowest numbers of clusters (Figure 1, Table 1), which means higher extent of aggregation. The number of intermolecular hydrogen bonds is very low and comparable for all systems (Table 1) suggesting that this type of molecular interaction does not explain the aggregation properties observed for peptides **5a-d**. The aggregation phenomenon seems to be better explained by the formation of intermolecular π-stacking interactions between the naproxen moiety and the aromatic amino acids.
Figure 2 shows the representative π-stacking interactions observed for compound **5b**.

View Article Online
DOI: 10.1039/C5TB00501A

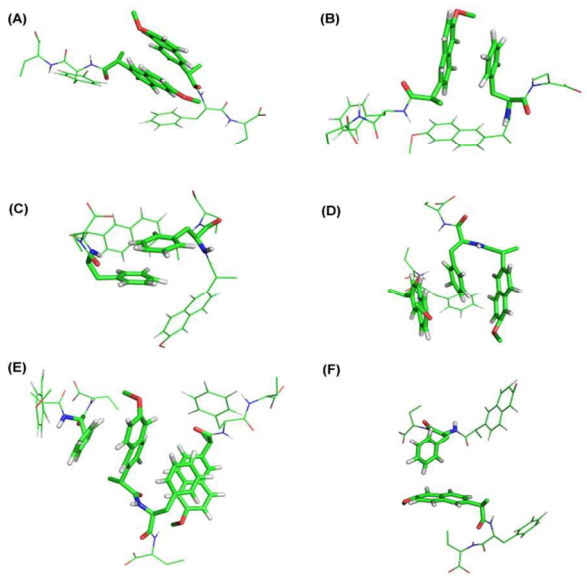

Figure 2. Illustration of representative π-stacking interactions observed for hydrogelator **5b** during the last 20 ns of the simulation. (A) Intermolecular interaction between the naproxen moieties, (B) Intermolecular interaction between Npx and Phe, (C) Intermolecular interaction between Phe groups, (D) Intra and intermolecular interactions, (E) Multiple intermolecular interactions and (F) T-shaped interaction between Phe and Npx.

Naproxen π-stacking, preferentially as the S type mode, occurs in all five dehydrodipeptides studied. PD π-stacking is also significant (Figure 2a). It is interesting to note that naproxen π-stacking alone cannot explain the aggregation phenomenon. Although peptide **5e** presents a high percentage of naproxen π-stacking interactions, the theoretical simulations suggest that this peptide is not able to self-aggregate (Figure 1). This leads to the conclusion that the sole intermolecular interaction between naproxen groups is not sufficient to promote peptide aggregation. On the other hand, the interactions between naproxen and other aromatic groups seem to be responsible for the aggregation of the peptides **5a-d**. Analyzing the systems of peptides **5a** or **5b** suggests that the self-aggregation phenomenon is determined by the intermolecular interaction between naproxen and the phenyl group of the aromatic amino acid (Figure 2b). The system containing peptide **5a** also suggests that the presence of two aromatic amino acid residues does not shows any additive effect on cluster formation, since the **5a** system shows less self-aggregation than **5b**. In fact, combining two aromatic residues such as phenylalanine and dehydrophenylalanine seems to have a detrimental effect on self-aggregation. The systems containing peptides **5c** and **5d**, indicate that self-aggregation in dehydrodipeptides with a single aromatic residue in the C-terminal position is less effective. Systems containing peptides **5a**, **5c** and **5d** also demonstrate that the dehydrophenylalanine residue does not establish significant intermolecular interactions with itself, instead, this amino acid seems to interact preferentially with naproxen. Furthermore, although **5c** and **5d** are structurally similar, **5c** shows a higher propensity to form clusters. This could result from the presence of valine that makes peptide **5c** less polar than peptide **5d**. From these results it is possible to conclude that the aggregation of this type of peptides is dominated by π-π interactions between the *N*-aromatic component and other aromatic amino acid moieties. Aromatic amino acid residues in addition to the N-aromatic capping group are required for peptide aggregation (as seen for **5e**).

Hydrogelation

Dehydrodipeptides **5a-e** were tested as hydrogelators in order to validate this methodology for the rational design of efficient hydrogelators. Gelation was triggered via pH change and/or heating and subsequent cooling. Compounds **5a** and **5b** were solubilized in PBS buffer at 60 ºC and gelation occurred upon cooling to room temperature (Figure 3). Compounds **5c** and **5d** were dissolved in water with addition of NaOH (1 M) and gelation occurred by pH adjustment with HCl (1 M) (Figure 3). The results showed that gelation of compounds **5a-d** occurs at low critical gelation concentrations (CGC), between 0.4 wt% and 0.8 wt% and gel-sol phase transition pH (pHgs) between 5 and 8 (Table 2).

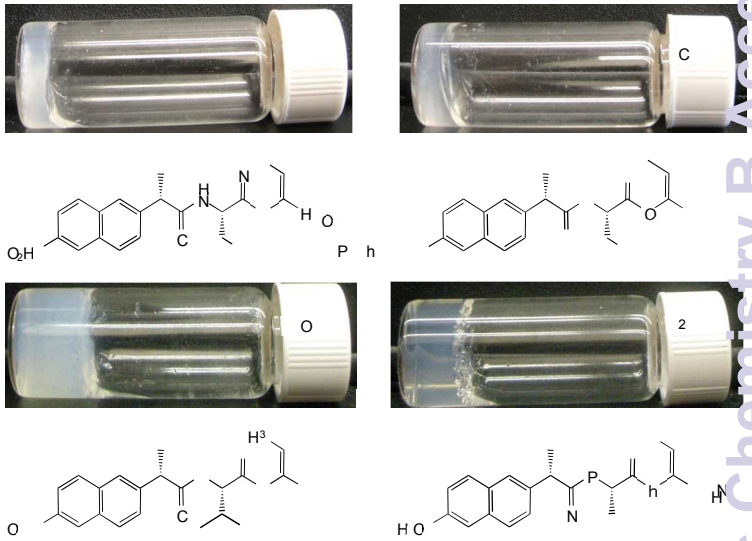

Figure 3. Optical images of hydrogels **5a-d.**

Table 2. CGC and gel-sol phase transition pH of compounds **5a-d**.

Compound	CGC [wt%]	pHgs
Npx-*L*-Phe-*Z*-ΔPhe-OH, **5a**	0.4	8.0
Npx-*L*-Phe-*Z*-ΔAbu-OH, **5b**	0.4	6.0
Npx-*L*-Val-*Z*-ΔPhe-OH, **5c**	0.6	8.0

Journal Name

View Article Online
DOI: 10.1039/C5TB00501A ARTICLE

Npx-*L*-Ala-*Z*-ΔPhe-OH, **5d**	0.8	5.0

As predicted by the molecular dynamic simulations, compound **5e** (Npx-L-Ala-*Z*-ΔAbu-OH), lacking an aromatic amino acid residue, failed to give a hydrogel in all conditions tested. The dehydropeptides with a capped *N*-terminal phenylalanine residue (**5a** and **5b**) display lower CGC compared to peptides **5c** and **5d**, bearing an alkyl N-terminal amino acid (Val or Ala). These experimental results are in excellent agreement with those obtained by the molecular dynamic simulations. This means that the molecular modelling methodology presented here might be a valuable new toll for the design of efficacious peptide hydrogelators..

Comparing the experimental conditions for hydrogelation of dehydrodipeptide **5a** with the dipeptide phenylalanylphenylalanine *N*-protected with naproxen (0.4 wt% and pH 8,0 *vs* 0.8 wt% and pH 7, respectivelly),[14] it is possible to conclude that the presence of the *α,β*-double bond decreases the CGC value and increases the gel-sol phase transition pH.

Hydrogelators **5a** and **5b**, containing different dehydroamino acids, dehydrophenylalanine and dehydroaminobutyric acid, respectively, were selected for further characterization, namely fluorescence studies, Circular Dichroism (CD) studies and proteolitic stability assays, to get insight into the effect of the structure of the dehydroaminoacid on the self-assembly and gelation processes and proteolitic stability. The properties of hydrogelator **5a** can be directly compared to its "natural" dipeptide analogue phenylalanylphenylalanine *N*-protected with Naproxen.[14]Moreover hydrogelator **5a** (bearing two aromatic amino acid residues) was expected to display fluorescence and CD spectra more insightful towards the self-assembly and gelation processes than **5c** and **5**d (containing only one aromatic amino acid residue). Rheological and Transmission Electron Microscopy (TEM) characterisation was carried out with gels **5a-d** (**5e** failed to produce a hydrogel).

Photophysical Studies

The critical aggregation concentration (CAC) as well as the influence of pH in the aggregation of peptides **5a** and **5b** were studied by fluorescence spectroscopy. Figure 4 shows the influence of pH in the fluorescence properties of molecules **5a** and **5b**. The fluorescence emission of peptides **5a** and **5b** is clearly dominated by the emission of the naproxen moiety, λ_{max}=353 nm (λ_{exc}= 290 nm), similar to the results reported for naproxen in methanol and water.[26] However, it is possible to observe a second fluorescence band, with maximum emission near 440 nm. This band is ascribed to the formation of an emissive dimmer between naproxen and the phenylalanine residues. At the excitation wavelength used (λ_{exc}= 290 nm), phenylalanine is not electronically excited.

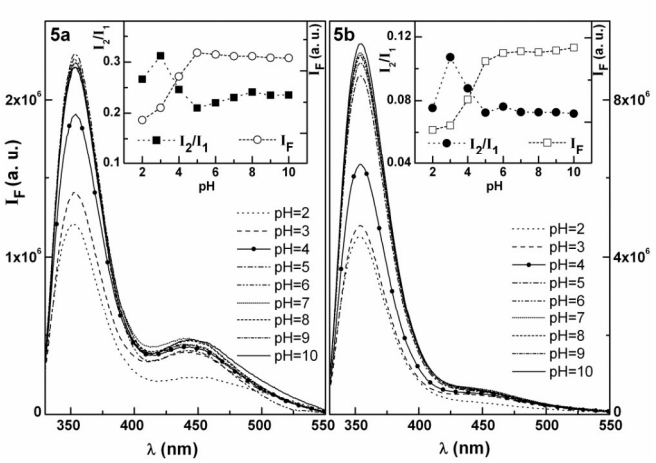

Figure 4. Fluorescence spectra of compounds **5a** and **5b** (2×10^{-6} M) at different pH values (λ_{exc}= 290 nm). Insets: Variation of the maximum fluorescence intensity and intensity ratio I_2/I_1 with pH.

For both compounds **5a** and **5b**, the maximum emission intensity rises with pH, with a tendency to stabilize for pH values above 5 for compound **5a** and 6 for compound **5b**. Considering the ratio between the aggregate band and naproxen monomer band, I_2/I_1, a different behaviour is observed: the maximum value of I_2/I_1 occurs at pH 3 for both compounds, near the pK_a value of the peptide terminal carboxylic acid group (pK_a~ 3)[27]. For both compounds, a minimum is observed at pH 5 with stabilization observed thereafter. A slight rise in I_2/I_1 ratio is observed at pH 8 for compound **5a** and pH 6 for compound **5b**, identified as the pH gelation values. The pH at which a gel is formed is highly dependent on the molecular structure of the hydrogelator and correlates with the apparent pK_a of the peptide.[28] The extent of deprotontion of the carboxylic acid group on the hydrogelators is pH-dependent and determines their hydrophilicity. Accordingly, compound **5b**, bearing only one aromatic amino acid, is more hydrophilic than **5a** (bearing two aromatic amino acid residues) thus requiring lower pH (pH= 6) for gelation comparing to **5a** (pH 8.0)

Excitation spectra provide relevant information about the nature of the aggregate emission band (Figure 5). It can be observed that upon collecting emission in the naproxen band (360 nm) or in the aggregate band (450 nm), the spectra completely modify showing different excited species, and not dynamic exciplexes formed at the excited state.

View Article Online
DOI: 10.1039/C5TB00501A
Journal Name

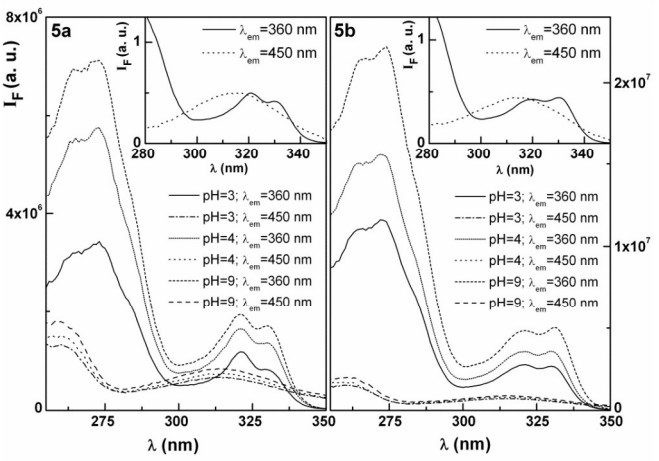

Figure 5. Excitation spectra (λ_{em}=360 nm and λ_{em}=450 nm) of compounds **5a** and **5b** (2×10^{-6} m) at selected representative pH values. Insets: Normalized spectra at the peak of minimum energy.

Figure 6 shows the dependence of fluorescence emission of compounds **5a** and **5b** with concentration.

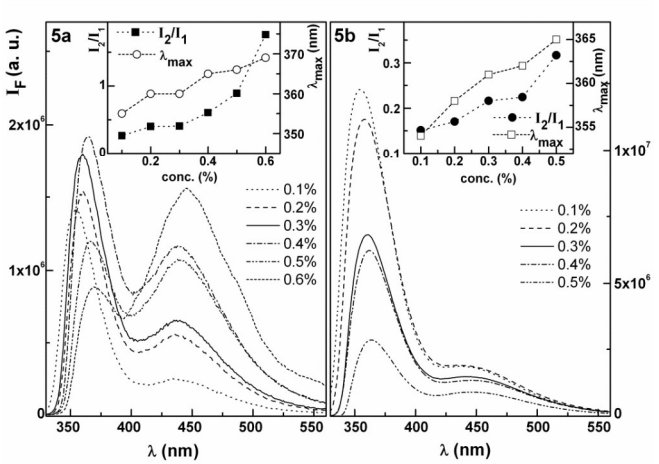

Figure 6. Fluorescence spectra of compounds **5a** (pH 8) and **5b** (pH 6) at several concentrations (λ_{exc}= 290 nm). Insets: Variation with concentration of the maximum emission wavelength of the first band and intensity ratio I_2/I_1.

It can be seen that the ratio of intensities of the aggregate and monomer bands, I_2/I_1 (insets of Figure 6), is almost constant for concentrations below 0.4 wt%, but increases sharply for higher concentrations. At this concentration, a clear change in the naproxen maximum emission wavelength is also detected, with a red shift that tends to stabilize at higher concentrations (inset of Figure 6, left). These results point clearly to hydrogel formation at 0.4 wt% for compound **5a**. For compound **5b**, the ratio I_2/I_1 follows the same trend (presenting lower values) with a noticeable rise above 0.4 wt%, as for compound **5a**. The red shift in naproxen emission with increasing hydrogelator concentration is smaller than that observed for compound **5a.** From these two indicators, a clear change in behaviour is detected above 0.4 wt%, pointing to hydrogel formation (inset of Figure 6, right). Above 0.4 wt% concentration, the aggregate emission band is clearly higher than what is observed at lower concentrations, which may indicate the formation of intermolecular aggregates that play an important role in gel formation.

These results show that fluorescence spectroscopy is a good methodology to estimate the critical gelation concentration and to get insight into the intramolecular/intermolecular interactions between the aromatic moieties of these molecules.

Hydrogel Characterization

The CD spectra of hydrogelators **5a** and **5b** and of the dipeptide Npx-phenylalanylphenylalanine (Npx-*L*-Phe-*L*-Phe-OH) were recorded in order to get insight into the peptide secondary structure (Figure 7).

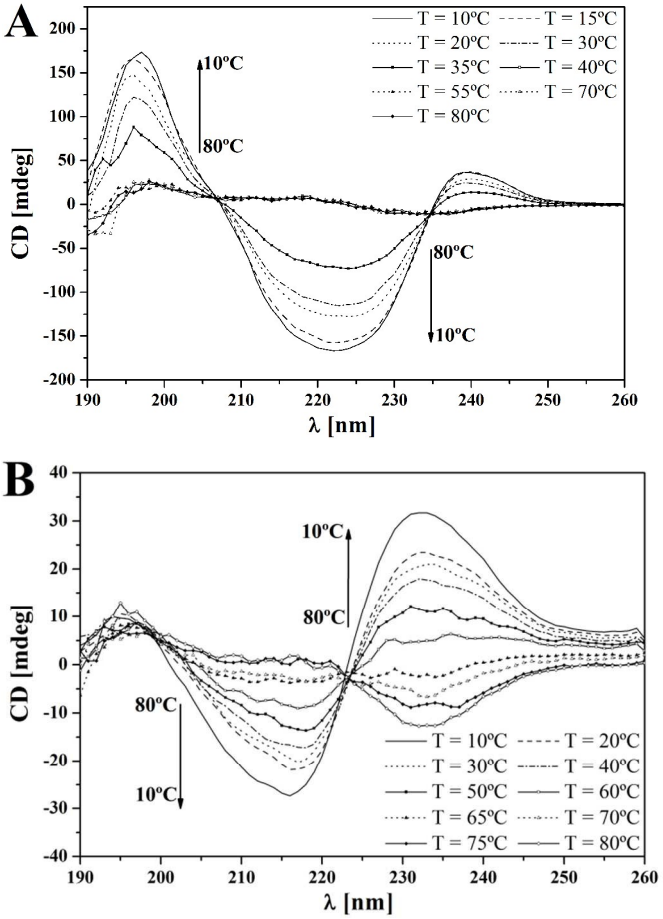

Journal Name View Article Online DOI: 10.1039/C5TB00501A ARTICLE

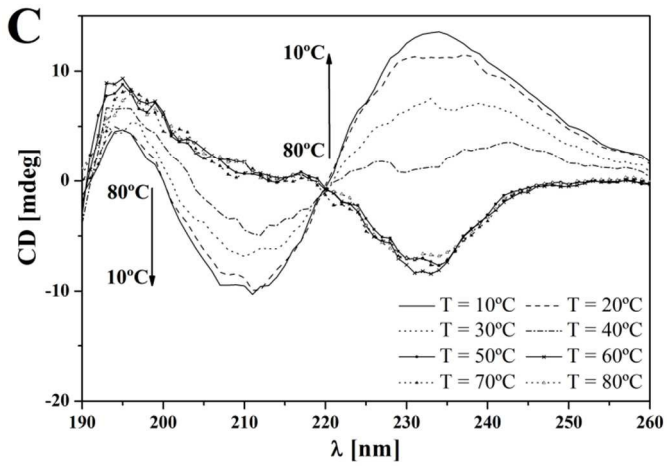

Figure 7. CD spectra of Npx-*L*-Phe-*L*-Phe-OH (A), Npx-Phe-ΔPhe-OH **5a** (B) and Npx-Phe-ΔAbu-OH **5b (**C).

The three peptides show similar CD spectra, displaying Cotton effects only in the far UV wavelength (190-260 nm). The CD spectra of Npx-*L*-Phe-*L*-Phe-OH (Figure 7A) at low temperatures exhibit bands around 196 nm (positive peak), 220 nm (broad negative peak) and 235 nm (positive Cotton effect). The signals at 196 nm and 220 nm indicate a *β*-sheet like arrangement of the peptide backbone, corresponding to π-π* and n-π* transitions, respectively.[29-34] The CD spectra of compounds **5a** and **5b** (Figure 7B and C) at low temperatures are similar to those obtained for Npx-*L*-Phe-*L*-Phe-OH. This suggests the same type of intermolecular interactions and *β*-sheet like structure. However, in Npx-*L*-Phe-*L*-Phe-OH the strongest bands are the ones resulting from the peptide backbone (195 nm and 220 nm), while in dehydrodipeptides **5a** and **5b**, the most intense bands originate from the naphthalene interactions (220 nm and 235 nm). This indicates that for the dehydrodipeptide hydrogelators the naphthalene interactions are more important than the peptide backbone arrangement. The variation of the CD spectra of these three compounds with temperature shows a progressive loss of structure up to 40 °C. For higher temperatures, the absence of CD signals suggests high mobility of the peptide backbone and the lack of an organized structure.[31] Cooling the peptide solutions leads to gelation, shown by the enhancement of the CD signals[31] and the blue shift of the λ_{max} of the bands. This indicates gradual transition from an isotropic solution to an anisotropic environment in the gel state.[35] In the case of Npx-*L*-Phe-*L*-Phe-OH, structure forming is abrupt and occurs at temperatures below 40 °C, where the signal strength increases rapidly as the temperature decreases. For compound **5a** the appearance of organized structures starts at a slightly higher temperature (around 60 ºC), suggesting that the dehydrophenylalanine residue increases the propensity for hydrogelation at higher temperatures. The hydrogelator **5b** showed a behaviour similar to that observed for Npx-*L*-Phe-*L*-Phe-OH. According to these results it is possible to conclude that the dehydrophenylalanine residue increases the hydrogel thermal stability.

Morphologycal analysis of the new hydrogels based on dehydrodipeptides was carried out using transmission electron microscopy (TEM). The TEM images of hydrogels obtained from compounds **5a-d** are shown in Figure 8.

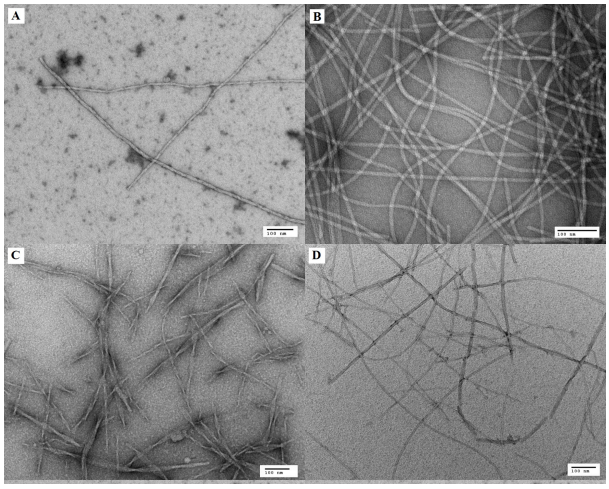

Figure 8. TEM images of hydrogels obtained from dehydrodipeptides (A) **5a**; (B) **5b**; (C) **5c**; (D) **5d** (scale bar of 100 nm).

Hydrogelator **5a** self-assembles into non-uniform nanofibers displaying different widths: minimum width of 9 nm and a maximum width of 18 nm, similar to those shown by Npx-*L*-Phe-*L*-Phe-OH.[14] Hydrogel **5b** exhibit long nanofibers, that entangle to form a network, with an average width of 10 nm. The nanofibers of hydrogelator **5c** are short (length between 170-750 nm) and non-uniform displaying a minimum width of 12 nm and maximum width of 16 nm. Hydrogel **5d** comprises long and entangled nanofibers with widths ranging between 8 and 16 nm.

The rheological data obtained with hydrogels **5a-d** are presented in Table 3.

Table 3. Rheological properties of hydrogels formed by naproxen-dehydropeptides **5a-d**.

Hydrogel [a]	Dynamic strain sweep			Dynamic frequency sweep	
	G'_{max} [Pa]	G''_{max} [Pa]	Critical strain [%]	$G'^{[b]}$ [Pa]	$G''^{[b]}$ [Pa]
5a	$1.6x10^3$	$2.2x10^2$	5.0	$1.7x10^3$	$2.2x10^2$
5b	$8.1x10^2$	92.7	1.6	$7.1x10^2$	79.3
5c	$5.9x10^2$	$1.1x10^2$	0.3	$6.6x10^2$	89.1
5d	$9.8x10^2$	$1.0x10^2$	8.0	$8.0x10^2$	$1.17x10^2$

[a] The concentration of the hydrogel is 0.4 wt% for compounds **5a** and **5b**, 0.6 wt% for compound **5c** and 0.8 wt% for compound **5d**. [b] The value is taken at 6.32 rad s^{-1}.

All hydrogels presented a storage modulus (G') significantly higher than their loss modulus (G'') and independent from frequency, which indicates a viscoelastic behaviour. The hydrogels of compounds **5d** and **5a** present the greater storage modulus and critical strains (8.0 % and 5.0 %, respectively), suggesting a more resilient network in these two hydrogels. Comparison between the critical strains of hydrogels of Npx-*L*-Phe-*Z*-ΔPhe-OH (**5a**), Npx-*L*-Phe-*L*-Phe-OH (0.62 %)[15] and Npx-*D*-Phe-*D*-Phe-OH (1.0 %)[14] shows that the *α*,*β*-double bond in **5a** increases the resistance of this gel to external force.

View Article Online
DOI: 10.1039/C5TB00501A Journal Name

Enzymatic and Toxicity Assays

The stability of the new dehydrodipeptide hydrogelators **5a** and **5b**, against proteolytic degradation with α-chymotrypsin was compared to Npx-*L*-Phe-*L*-Phe-OH (Figure 9). α-Chymotrypsin was chosen for its ability to preferentially cleave peptide amide bonds where the carboxyl side of the amide bond is an aromatic amino acid. Thus, the peptide bond between the Phe residues on the control substrate Npx-***L*-Phe-*L*-Phe**-OH and the peptide bond between the Phe residue and the dehydroamino acid residue in peptides **5a** (Npx-***L*-Phe-*Z*-ΔPhe**-OH) and **5b** (Npx-***L*-Phe-*Z*-ΔAbu**-OH) are the likely clevage sites for chymotripsin. Dehydropeptides **5c (**Npx-***L*-Val-*Z*-ΔPhe**-OH**)** and **5d (**Npx-***L*-Ala-*Z*-ΔPhe**-OH**)** lacking an aromatic amino acid residue in position P1 are not likelly to be recognized by chymotrypsin as substrates. The results show that while the control substrate Npx-***L*-Phe-*L*-Phe**-OH undergoes fast proteolytic degradation, the dehydrodipeptides **5a** and **5b** are completely stable when treated with α-chymotrypsin for 80 hrs (Figure 9). The capping *N*-terminal amide bond of naproxen on peptides **5a** and **5b** was also found stable towards chymotripsin-catalysed hydrolysis.

Replacement of the *C*-termimal Phe residue on the control substrate by a dehydroamino acid rends that peptide bond resistant to hydrolysis.

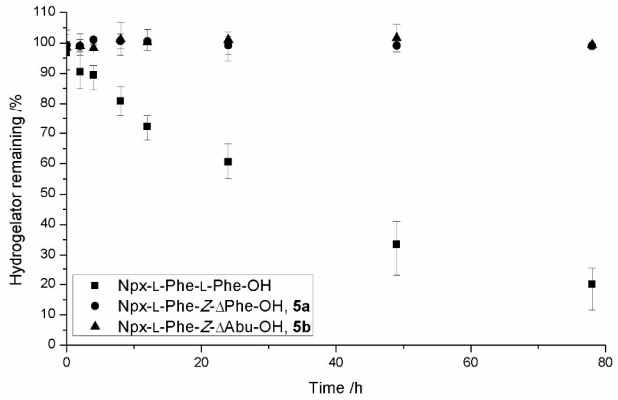

Figure 9. Evaluation of the proteolitic stability of hydrogelators Npx-*L*-Phe-*L*-Phe-OH; Npx-*L*-Phe-*Z*-ΔPhe-OH, **5a** and Npx-*L*-Phe-*Z*-ΔAbu-OH, **5b** in the presence of *α*-chymotrypsin (pH 7.4, 25 ºC).for 80 hours.

A preliminary evaluation of the cellular toxicity of the dehydrodipeptide hydrogelators was carried out on adult human skin fibroblasts.

Cell viability after incubation for 48 hrs with 50 μM, 100 μM and 500 μM of hydrogelator **5d** is presented in figure 10. The dehydrodipeptide did not show toxicity, even at concentrations as high as 500 μM. Hydrogelator **5d** was selected for testing due to its higher solubility at 37 ºC in the cell culture medium, comparing to hydrogelators **5a-c,** thanks to its relatively high CGD (presumably substantially higher at physiological pH). This allowed studying the effect of the hydrogelator on cellular viability in a wide range of concentrations, up to 500 μM, without potential interference from nano/microstructures that form before macroscopic gel formation can be detected. For relevant biological applications the biocompatibility of the hydrogels, needs also to be assessed. The biocompatibility of the hydrogels as cell culture media will be evaluated in the near future.

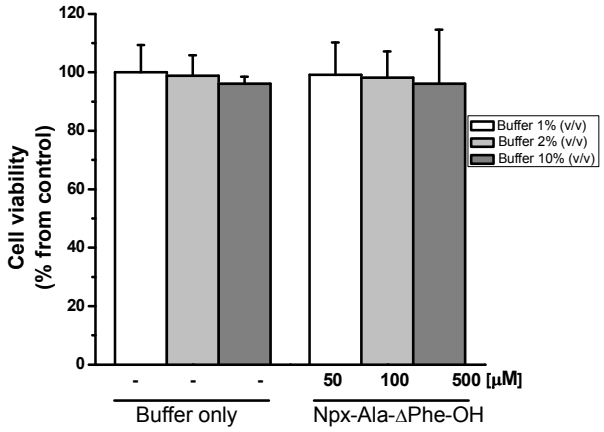

Figure 10. Cell viability of adult human skin fibroblasts after incubation for 48 h with 50 μM, 100 μM or 500 μM of Npx-*L*-Ala-*Z*-ΔPhe-OH (**5d**), as compared with buffer controls. No significant differences were observed (P>0.05).

Experimental

Melting points (ºC) were determined in a Gallenkamp apparatus and are uncorrected. ^{1}H and ^{13}C NMR spectra were recorded on a Bruker Avance III at 400 and 100.6 MHz, respectively, or in a Varian Unity Plus 300 at 300 and 75.4 MHz, respectively. ^{1}H–^{1}H spin–spin decoupling and DEPT θ 45º were used. HMQC and HMBC were used to attribute some signals. Chemical shifts (δ) are given in parts per million (ppm) and coupling constants (*J*) in hertz (Hz). High resolution mass spectrometry (HRMS) data were recorded by the mass spectrometry service of the University of Vigo, Spain. Elemental analysis was performed on a LECO CHNS 932 elemental analyzer. Column chromatography was performed on Macherey–Nagel silica gel 230–400 mesh. Petroleum ether refers to the boiling range 40–60 °C.

Transmission Electron Microscopy (TEM): TEM images were recorded on a Morgagni 268 Transmission Electron Microscope operating at 80 kV. The samples were prepared using the uranyl acetate negative staining method. In a carbon coated copper grid (400 mesh), 4 μL of the hydrogel was placed and left for 30 seconds. The excess of water from the hydrogel was removed using filter paper, and washed with water and a solution of uranyl acetate (2 %) (3 times each).

Rheometry: Rheological studies were performed on a ARES-G2 rheometer with a parallel plate at 25 ºC. Dynamic strain sweep and frequency sweep experiments were carried out. During the strain sweep experiments the hydrogels were under different oscillation strain, constant frequency (6.28 rad/s) and

Journal Name View Article Online DOI: 10.1039/C5TB00501A ARTICLE

constant temperature (25.5 ºC). In a frequency sweep, the experiments were carried out under different frequencies (0.1 to 200 rad/s), constant oscillation amplitude and temperature (25.5 ºC).

CD spectroscopy: The CD spectra were obtained in an OLIS DSM-20 CD spectropolarimeter operating in the UV-Visible spectral region, equipped with a Peltier temperature control unit. The near UV spectra (500-260 nm) were obtained with 1 second accumulations every 1 nm. The far UV spectra (260-190 nm) were obtained with 5 seconds accumulations every 1 nm. Optical cells with path lengths ranging from 0.05 to 1.00 mm were used. Baselines with the buffer used in each hydrogel were obtained at 20 ºC and 80 ºC. As no relevant differences in the spectra were observed with the variation of temperature, the hydrogels spectra were corrected with the baselines at 20 ºC. Correction in relation to the path length of the optical cell used was also made. The data were smoothed mathematically in Origin 8 software. The optical cells were filled with each hydrogel pre-heated at 80 ºC to form a clear solution, and then introduced in the CD spectropolarimeter with the temperature previously programmed to 80 ºC. The spectra were obtained 10-15 minutes after each change in temperature.

Photophysical studies: Fluorescence measurements were performed using a Fluorolog 3 spectrofluorimeter, equipped with double monochromators in both excitation and emission, Glan-Thompson polarizers and a temperature controlled cuvette holder. Fluorescence emission and excitation spectra were corrected for the instrumental response of the system.

Molecular Dynamic Simulations: The molecular structure of the peptides **5a-e** with unnatural *α,β*-dehydroamino acids under study (Scheme 1) were designed with the program Pymol.[25] These molecules were parameterized using parameters transferred from the natural amino acids in the GROMOS 54a7[36,37] force field. To validate the proposed parameters, the new amino acids were subjected to 12000 steps of energy minimization calculations with the steepest descent algorithm and 100 ps MD simulation in a cubic box solvated with Simple Point Charge (SPC) water model.[23] The validation was done by analyzing the convergence of the system's potential energy and the geometry of the amino acids. The naproxen group present in all five peptides under study **5a-e** was also parameterized according to the GROMOS54a7 force field and the molecule was subjected to the same protocol used to validate the *α,β*-dehydroamino acids. The topologies of Npx, ΔPhe and ΔAbu are available upon request. The five peptides **5a-e** were designed and eleven copies were placed in a cubic box of size 4.5 x 4.5 x 4.5 nm solvated with SPC water model.[23] Each system was energy minimized with the steepest descent algorithm and 60 ns of MD simulations were run, the first 40 ns were spent for equilibration and the last 20 ns were used for analysis. In these experiments the simulation was made in 30000000 steps with integration interval of 2 fs. All simulations were run with the GROMACS 4.5.4 software package.[38,39] In all MD simulations the system was maintained at constant temperature and pressure of 310 K and 1 atm, respectively, using the Berendsen thermostat and barostat methods,[40] with $\tau_T = 0.20$ ps and $\tau_P = 0.10$ ps. The SETTLE algorithm[41] was used to constrain bond lengths and angles of water molecules, while the bond lengths and angles of peptides were constrained with LINCS algorithm.[42] For the treatment of long-range interactions, we used the reaction field method, with cut-off of 1.4 nm and dielectric constant of ε = 54 for water. The Van der Waals interactions were also calculated with a cut-off radius of 1.4 nm. The aggregation properties of each peptide system were evaluated by identifying the occurrence of peptide clusters formed in the simulation box. Peptide clusters were detected by clustering peptides using the single-linkage method with a cut-off of 1.4 nm between the center of mass of each peptide. The number of clusters for each system was counted and characterized. The average number of intra and intermolecular hydrogen bonds, and also the average number of intra and intermolecular *π*-stacking interactions were calculated in order to understand the interactions responsible for the formation of the aggregates.

Enzymatic resistance assay: To illustrate the enzymatic resistance of dehydrodipeptides, diluted solutions of compounds **5a** and **5b** and of Npx-*L*-Phe-*L*-Phe-OH (0.5 mg mL^{-1}) were prepared in sodium phosphate buffer pH 7.47 0.1 M and divided in three samples of 100 µL. A solution of *α*-chymotrypsin in the same buffer was also prepared (1.0 mg mL^{-1}). All the solutions were incubated at 37 ºC and 20 rpm overnight. The enzyme solution (100 µL) was added to each hydrogelator solution. Samples of 10 µL were taken at 0 h, 2 h, 4 h, 8 h, 12 h, 24 h, 49 h and 78 h. and analyzed by HPLC (λ= 276 nm; water/acetonitrile, 1:1 with 0.1 % TFA). The percentage of gelator was determined using the peptide peak area in each sample and comparing it with the area of the same peak in the diluted solutions without the enzyme. To verify that these solutions were stable at 37 ºC, samples of each peptide were analyzed by HPLC after 78 hours at 37 ºC and 20 rpm.

MTT assay: Adult human skin fibroblasts (ASF-2 cells) were maintained at 37 ºC in a humidified 5 % CO_2 atmosphere grown in Dulbecco´s Modified Eagle's Medium (DMEM, Sigma-Aldrich, St. Louis, MO, USA) supplemented with 10 % Fetal bovine serum (FBS, Lonza, Verviers, Belgium), 10 mM Hepes and 1 % antibiotic/antimycotic solution (Sigma-Aldrich, St. Louis, MO, USA). Prior to culture, cells within a sub-confluent monolayer were trypsinized using trypsin (0.05 %)-EDTA.4Na (0.53 mM) solution and resuspended in DMEM to obtain a cell concentration of around 50,000 cells per mL. The cells were plated in 96-multiwell culture plates (100 µL/well) 24 hours before incubation with compound **5d**. Cells were then treated with different concentrations of **5d**, prepared as follow: Npx-L-Ala-*Z*-ΔPhe-OH (**5d**) was dissolved in phosphate buffer 0.1 M pH 8, obtaining a solution of 5.0 mM. The 5 mM solution was used to prepare solutions of 50 µM, 100 µM and 500 µM in DMEM. Solutions of phosphate buffer 0.1 M pH 8 at 1 %, 2 % and 10 % in DMEM were prepared as controls. 100 µL aliquots of buffer controls and **5d** solutions were placed into the wells of the plate with the cell culture, with three replicas of each. The plate was incubated at 37 ºC for 48 hours. Cells were then incubated for 60 minutes with MTT [3-(4,5-

View Article Online
DOI: 10.1039/C5TB00501A
Journal Name

dimethylthiazol-2-yl)-2,5-diphenyltetrazolium bromide, Sigma-Aldrich, St. Louis, MO, USA] to a final concentration of 0.5 mg mL^{-1}. Then, the medium was removed, and the formazan crystals formed by the cell's capacity to reduce MTT were dissolved with a 50:50 (v/v) DMSO:ethanol solution, and absorbance measured at 570 nm (with background subtraction at 690 nm), in a SpectroMax Plus384 absorbance microplate reader. The results were expressed as percentage relative to the control (cells with buffer solution).

*Synthesis of β-hydroxydipeptides derivatives (**1a-e**):* The synthesis of compound **1a**,[43] **1b**[43] and **1e**[16] was described elsewhere.

*Synthesis of Boc-L-Val-D,L-Phe(β-OH)-OMe (**1c**):* Boc-L-Val-OH (4.34 g, 20 mmol) was treated with H-D,L-Phe(*β*-OH)-OMe,HCl (4.63 g, 20 mmol) in acetonitrile using the standard *N,N'*-dicyclohexylcarbodiimide (DCC)/ 1-hydroxybenzotriazole (HOBt) procedure, giving **1c** (6.89 g, 87 %) as an oil; ^{1}H NMR (300 MHz, $CDCl_3$, δ): 0.60-0.67 (dd, *J* = 6.3 and 7.2 Hz, 6H, *γ*CH_3 Val), 0.79-0.89 (dd, *J* = 6.9 and 9.2 Hz, 6H, *γ*CH_3 Val), 1.40 (s, 18H, CH_3 Boc), 1.83–2.00 (m, 2H, *β*CH Val), 3.72 (s, 3H, OCH_3), 3.73 (s, 3H, OCH_3), 3.77-3-97 (m, 2H, *α*CH Val), 4.86-4.92 [m, 2H, *α*CH Phe(*β*-OH)], 5.01-5.14 (dd, *J* = 9.0 and 21 Hz, 2H, NH Val), 5.30-5.38 [dd, *J* = 4.0 and 28.4 Hz, 2H, *β*CH Phe(*β*-OH)], 7.09-7.16 [m, 2H, NH Phe(*β*-OH)], 7.20–7.39 (m, 10H, Ar H); ^{13}C NMR (75.4 MHz, $CDCl_3$, δ): 17.14 (*γ*CH_3 Val), 17.74 (*γ*CH_3 Val), 18.99 (*γ*CH_3 Val), 28.20 (CH_3 Boc), 30.86 (*β*CH Val), 52.47 (OCH_3), 52.58 (OCH_3), 58.04 [*α*CH Phe(*β*-OH)], 58.22 [*α*CH Phe(*β*-OH)], 59.48 (*α*CH Val), 59.78 (*α*CH Val), 73.00 [*β*CH Phe(*β*-OH)], 73.47 [*β*CH Phe(*β*-OH)], 79.91 [$(CH_3)_3C$], 125.64 (CH), 125.86 (CH), 127.75 (CH), 127.81 (CH), 128.25 (CH), 128.30 (CH), 139.73 (C), 139.78 (C), 155.89 (C=O), 155.94 (C=O), 170.73 (C=O), 170.99 (C=O), 171.90 (C=O), 172.01 (C=O); HRMS (ESI) *m/z*: $[M + Na]^+$ calcd for $C_{20}H_{30}N_2NaO_6$ 417.19961; found, 417.19957.

*Synthesis of Boc-L-Ala-D,L-Phe(β-OH)-OMe (**1d**):* Boc-*L*-Ala-OH (1.89 g, 10 mmol) was treated with H-*D,L*-Phe(*β*-OH)-OMe,HCl (2.32 g, 10 mmol) in acetonitrile using the standard DCC/HOBt procedure, giving **1d** (3.50 g, 95 %) as an oil; ^{1}H NMR (300 MHz, $CDCl_3$, δ): 1.10-1.25 (m, 6H, *β*CH_3 Ala), 1.40 (2s, 9H, CH_3 Boc), 1.42 (2s, 9H, CH_3 Boc), 3.35 (brs, 2H, OH), 3.71 (2s, 3H, OCH_3), 3.73 (2s, 3H, OCH_3), 4.14 (brs, 2H, *α*CH Ala), 4.84-4.88 [dd, *J* = 3.3 and 7.2 Hz, 2H, *α*CH Phe(*β*-OH)], 5.08 (brs, 1H, NH Ala), 5.18 (brs, 1H, NH Ala), 5.26-5.30 [dd, *J* = 3.0 and 6.6 Hz, 2H, *β*CH Phe(*β*-OH)], 7.12 [brd, *J* = 8.7 Hz, 2H, NH Phe(*β*-OH)], 7.24–7.37 (m, 10H, Ar H); ^{13}C NMR (75.4 MHz, $CDCl_3$, δ): 18.20 (*β*CH_3 Ala), 18.53 (*β*CH_3 Ala), 28.21 (CH_3 Boc), 49.84 (*α*CH Ala), 52.52 (OCH_3), 52.59 (OCH_3), 58.09 [*α*CH Phe(*β*-OH)], 73.33 [*β*CH Phe(*β*-OH)], 73.55 [*β*CH Phe(*β*-OH)], 80.04 [$(CH_3)_3C$], 125.77 (CH), 125.90 (CH), 127.90 (CH), 128.24 (CH), 128.26 (CH), 139.67 (C), 155.39 (C=O), 155.42 (C=O), 170.77 (C=O), 170.96 (C=O), 172.93 (C=O); HRMS (ESI) *m/z*: $[M + Na]^+$ calcd for $C_{18}H_{26}N_2NaO_6$ 389.16831; found, 389.16827.

*Synthesis of dehydrodipeptides derivatives (**2a-e**):* DMAP (0.1 equiv) was added to solutions of compounds **1a-e** in dry acetonitrile (1 M) followed by Boc_2O (1.0 equiv) under rapid stirring at room temperature. The reaction was monitored by ^{1}H NMR until all the reactant had been consumed. Then TMG (2 % in volume) was added, stirring was continued and the reaction followed by ^{1}H NMR. When all the reactant had been consumed, evaporation at reduced pressure gave a residue that was partitioned between ethyl acetate (50 mL) and $KHSO_4$ (30 mL, 1 M). The organic phase was thoroughly washed with $KHSO_4$ (1 M) and brine (2x30 mL, each), and dried with $MgSO_4$. Removal of the solvent afforded compounds **2a-e**.

The synthesis of compounds **2a**[43], **2b**[44] and **2e**[45] was described elsewhere.

*Synthesis of Boc-L-Val-Z-ΔPhe-OMe (**2c**):* Compound **1c** (1.97 g, 5 mmol) was treated according to the procedure described above to give compound **2c** (1.70, 90 %) as a white solid; mp 152.0-153.0 ºC; ^{1}H NMR (300 MHz, $CDCl_3$, δ): 1.00 (dd, *J* = 6.6 Hz, 6H, *γ*CH_3 Val), 1.44 (s, 9H, CH_3 Boc), 2.18–2.28 (m, 1H, *β*CH Val), 3.81 (s, 3H, OCH_3), 4.01-4.16 (m, 1H, *α*CH Val), 5.14 (d, *J* = 9.0 Hz, 1H, NH Val), 7.28–7.35 (m, 3H, Ar H), 7.34 (s, 1H, *β*CH ΔPhe), 7.48 (d, *J* = 6.9 Hz, 2H, Ar H), 7.81 (s, 1H, NH ΔPhe); ^{13}C NMR (75.4 MHz, $CDCl_3$, δ): 17.56 (*γ*CH_3 Val), 19.26 (*γ*CH_3 Val), 28.25 (CH_3 Boc), 30.49 (*β*CH Val), 52.50 (OCH_3), 59.99 (*α*CH Val), 80.04 [$(CH_3)_3C$], 123.96 (C), 128.53 (CH), 129.43 (C), 129.70 (CH), 132.66 (CH), 133.44 (*β*CH ΔPhe), 155.96 (C=O), 165.40 (C=O), 170.72 (C=O); Anal. calcd for $C_{20}H_{28}N_2O_5$: C 63.81, H 7.50, N 7.44; found: C 63.36, H 7.36, N 7.40.

*Synthesis of Boc-L-Ala-Z-ΔPhe-OMe (**2d**):* Compound **1d** (3.50 g, 9.5 mmol) was treated according to the procedure described above to give compound **2d** (3.05 g, 92 %,) as a white solid; mp 107.0-108.0 ºC; ^{1}H NMR (300 MHz, $CDCl_3$, δ): 1.38-1.44 (m, 12H, *β*CH_3 Ala and CH_3 Boc), 3.79 (s, 3H, OCH_3), 4.36 (brs, 1H, *α*CH Ala), 5.27 (brs, 1H, NH Ala), 7.28–7.36 (m, 3H, Ar H), 7.40 (s, 1H, *β*CH ΔPhe), 7.47 (d, *J* = 6.6 Hz, 2H, Ar H), 8.02 (s, 1H, NH ΔPhe); ^{13}C NMR (75.4 MHz, $CDCl_3$, δ): 17.87 (*β*CH_3 Ala), 28.22 (CH_3 Boc), 50.22 (*α*CH Ala), 52.55 (OCH_3), 80.19 [$(CH_3)_3C$], 123.79 (*α*C), 128.46 (CH), 129.44 (CH), 129.71 (CH), 133.20 (*β*CH ΔPhe), 133.46 (C), 155.58 (C=O), 165.46 (C=O), 171.54 (C=O); HRMS (ESI) *m/z*: $[M + Na]^+$ calcd for $C_{18}H_{24}N_2NaO_5$ 371.15774; found, 371.15774.

*Synthesis of dehydrodipeptides **3a-e**:* TFA (0.3 M) was added to compounds **2a-e**. After 2 hours the mixture was taken to dryness at reduced pressure to afford the corresponding dehydrodipeptide methyl ester.

*Synthesis of H-L-Phe-Z-ΔPhe-OMe,TFA (**3a**):* The general procedure described above was followed using compound **2a** (0.86 g, 1.95 mmol) giving compound **3a** (0.79 g, 92 %) as a white solid; mp 87.0-88.0 ºC; ^{1}H NMR (400 MHz, DMSO-d_6, δ): 2.94–3.00 (dd, *J* = 9.2 and 5.2 Hz, 1H, *β*CH_2 Phe), 3.24–3.29 (dd, *J* = 4.8 and 9.2 Hz, 1H, *β*CH_2 Phe), 3.73 (s, 3H, OCH_3), 4.25 (brs, 1H, *α*CH Phe), 7.30–7.41 (m, 9H, Ar H and *β*CH ΔPhe), 7.58-7.60 (dd, *J* = 2.0 and 4.0 Hz, 2H, Ar H), 8.26 (brs, 3H, NH_3^+), 10.37 (s, 1H, NH ΔPhe); ^{13}C NMR (100.6 MHz, DMSO-d_6, δ): 36.69 (*β*CH_2 Phe), 52.37 (OCH_3), 53.61 (*α*CH Phe), 125.03 (*α*C), 127.31 (CH), 128.64 (CH), 128.71 (CH), 129.57 (CH), 129.72 (CH), 130.01 (CH), 132.31 (*β*CH

Journal Name

View Article Online
DOI: 10.1039/C5TB00501A ARTICLE

ΔPhe), 132.83 (C), 134.80 (C), 164.87 (C=O), 168.30 (C=O); HRMS (micrOTOF) *m/z*: $[M]^+$ calcd for $C_{19}H_{21}N_2O_3^+$ 325.15467; found, 325.15545.

*Synthesis of H-L-Phe-Z-ΔAbu-OMe,TFA (**3b**):* The general procedure described above was followed with compound **2b** (1.74 g, 4.8 mmol) giving compound **3b** (1.60 g, 89 %) as an oil; ^{1}H NMR (400 MHz, DMSO-d_6, δ): 1.60 (d, J = 7.2 Hz, 3H, γCH_3 ΔAbu), 2.99-3.05 (dd, J = 8.0 and 6.0 Hz, 1H, βCH_2), 3.14-3.19 (dd, J = 6.0 and 8.0 Hz, 1H, βCH_2 Phe), 3.66 (s, 3H, OCH_3), 4.18-4.20 (m, 1H, αCH Phe), 6.60 (q, J = 7.2 Hz, 1H, βCH ΔAbu), 7.27-7.34 (m, 5H, Ar H), 8.29 (brs, 3H, NH_3^+), 9.89 (s, 1H, NH ΔAbu); ^{13}C NMR (100.6 MHz, DMSO-d_6, δ): 13.45 (γCH_3 ΔAbu), 37.04 (βCH_2 Phe), 52.00 (OCH_3), 53.41 (αCH Phe), 126.71 (αC), 127.22 (CH), 128.57 (CH), 129.57 (CH), 133.68 (βCH ΔAbu), 134.74 (C), 164.11 (C=O), 167.22 (C=O); HRMS (micrOTOF) *m/z*: $[M]^+$ calcd for $C_{14}H_{19}N_2O_3^+$ 263.13902; found, 263.13925.

*Synthesis of H-L-Val-Z-ΔPhe-OMe,TFA (**3c**):* The general procedure described above was followed with compound **2c** (0.75 g, 2.0 mmol) giving compound **3c** (0.70 g, 90 %) as a white solid; mp 228.5-230.0 ºC; ^{1}H NMR (300 MHz, DMSO-d_6, δ): 0.98 (d, J = 6.9 Hz, 3H, γCH_3 Val), 1.04 (d, J = 6.9 Hz, 3H, γCH_3 Val), 2.19-2.30 (m, 1H, βCH Val), 3.71 (s, 3H, OCH_3), 3.82 (brs, 1H, αCH Val), 7.31 (s, 1H, βCH ΔPhe), 7.36-7.48 (m, 3H, Ar H), 7.65-7.69 (m, 2H, Ar H), 8.27 (brs, 3H, NH_3^+ Val), 10.25 (brs, 1H, NH ΔPhe); ^{13}C NMR (75.4 MHz, DMSO-d_6, δ): 16.98 (γCH_3 Val), 18.31 (γCH_3 Val), 29.91 (βCH Val), 52.26 (OCH_3), 57.35 (αCH Val), 125.30 (αC), 128.68 (CH), 129.74 (CH), 130.17 (CH), 132.43 (βCH ΔPhe), 132.87 (C), 164.88 (C=O), 168.32 (C=O); Anal. calcd for $C_{17}H_{21}N_2O_5F_3$: C 52.31, H 5.42, N 7.18; found: C 51.83, H 5.47, N 7.19.

*Synthesis of H-L-Ala-Z-ΔPhe-OMe,TFA (**3d**):* The general procedure described above was followed with compound **2d** (1.39 g, 4.0 mmol) giving compound **3d** (1.33 g, 95 %) as an oil; ^{1}H NMR (300 MHz, DMSO-d_6, δ): 1.46 (d, J = 6.9 Hz, 3H, βCH_3 Ala), 3.72 (s, 3H, OCH_3), 4.08 (brt, J = 5.7 Hz, 1H, αCH Ala), 7.37–7.42 (m, 4H, Ar H and βCH ΔPhe), 7.63-7.67 (m, 2H, Ar H), 8.28 (brs, 3H, NH_3^+), 10.17 (s, 1H, NH ΔPhe); ^{13}C NMR (75.4 MHz, $CDCl_3$, δ): 16.77 (βCH_3 Ala), 48.44 (αCH Ala), 52.44 (OCH_3), 125.16 (αC), 128.76 (CH), 129.88 (CH), 130.12 (CH), 133.03 (C), 133.29 (βCH ΔPhe), 164.99 (C=O), 169.70 (C=O).

*Synthesis of H-L-Ala-Z-ΔAbu-OMe,TFA (**3e**):* The general procedure described above was followed with compound **2e** (0.69 g, 2.4 mmol) giving compound **3e** (0.60 g, 86 %) as an oil; ^{1}H NMR (300 MHz, DMSO-d_6, δ): 1.42 (d, J = 6.9 Hz, 3H, βCH_3 Ala), 1.69 (d, J = 7.5 Hz, 3H, γCH_3 ΔAbu), 3.66 (s, 3H, OCH_3), 3.99 (brs, 1H, αCH Ala), 6.66 (q, J = 6.9 Hz, 1H, βCH ΔAbu), 8.19 (brs, 3H, NH_3^+), 9.74 (s, 1H, NH ΔAbu); ^{13}C NMR (75.4 MHz, $CDCl_3$, δ): 13.49 (γCH_3 ΔAbu), 17.18 (βCH_3 Ala), 48.25 (αCH Ala), 52.07 (OCH_3), 125.83 (αC), 134.03 (βCH ΔAbu), 164.13 (C=O), 168.81 (C=O).

*Synthesis of dehydrodipeptides **4a-e**:* Triethylamine (2.2 equiv) was added to a solution of dehydrodipeptide methyl ester hydrochloride (**3a-e**) in dichloromethane (0.1 M), and (S)-(+)-naproxen chloride (1 equiv) was then slowly added with vigorous stirring and cooling in an ice bath. After stirring at 0 °C for 30 minutes the solution was stirred at room temperature overnight. The reaction mixture was then concentrated and partitioned between ethyl acetate (100 mL) and $KHSO_4$ (1 M, 50 mL) and washed with $KHSO_4$ (1 M), $NaHCO_3$ (1 M) and brine (3x30 mL). After drying over $MgSO_4$ the extract was taken to dryness at reduced pressure to afford the corresponding *N*-protected dehydrodipeptide methyl ester (**4a-e**).

*Synthesis of compound Npx-L-Phe-Z-ΔPhe-OMe (**4a**):* The general procedure described above was followed with compound **3a** (0.40 g, 0.91 mmol) giving compound **4a** (0.35 g, 71 %) as a white solid; mp 176.0-177.0 ºC; ^{1}H NMR (400 MHz, $CDCl_3$, δ): 1.52 (d, J = 7.2 Hz, 3H, CH_3), 2.95-3.01 (dd, J = 7.6 Hz, 1H, βCH_2 Phe), 3.08-3.12 (dd, J = 6.4 Hz, 1H, βCH_2 Phe), 3.64 (q, J = 7.2 Hz, 1H, CH), 3.72 (s, 3H, OCH_3), 3.93 (s, 3H, OCH_3), 4.82 (q, J = 7.6 Hz, 1H, αCH Phe), 5.96 (d, J = 8.0 Hz, 1H, NH Phe), 7.04 (d, J = 7.8 Hz, 2H, Ar H), 7.09 (d, J = 2.4 Hz, 2H, Ar H), 7.11-7.23 (m, 7H, Ar H), 7.30-7.32 (m, 3H, Ar H), 7.51 (s, 1H, □-CH), 7.61 (dd, J = 8.4 and 8.8 Hz, 2H, Ar H), 7.77 (brs, 1H, NH ΔPhe); ^{13}C NMR (100.6 MHz, $CDCl_3$, δ): 18.10 (CH_3), 36.80 (βCH_2 Phe), 46.85 (αCH Phe), 52.50 (OCH_3), 54.41 (CH), 55.28 (OCH_3), 105.59 (CH), 119.15 (CH), 123.72 (CH), 125.94 (CH), 126.17 (CH), 126.90 (CH), 127.17 (CH), 127.69 (CH), 128.58 (CH), 128.93 (C), 129.21 (CH), 129.27 (C), 129.42 (CH), 129.66 (CH), 132.70 (CH), 133.29 (C), 133.81 (C), 135.21 (C), 136.05 (C), 157.80 (C-O), 165.14 (C=O), 169.70 (C=O), 175.07 (C=O); Anal. calcd for $C_{33}H_{32}N_2O_5$: C 73.86, H 6.01, N 5.22; found: C 73.45, H 6.023, N 4.924.

*Synthesis of Npx-L-Phe-Z-ΔAbu-OMe (**4b**):* The general procedure described above was followed with compound **3b** (0.438 g, 1 mmol) giving compound **4b** (0.433 g, 91 %) as a white solid; mp164.0-165.0 ºC; ^{1}H NMR (400 MHz, $CDCl_3$, δ): 1.52-1.56 (m, 6H, CH_3 and γCH_3 ΔAbu), 2.96-3.01 (dd, J = 7.6 Hz, 1H, βCH_2 Phe), 3.10-3.15 (dd, J = 6.4 Hz, 1H, βCH_2 Phe), 3.64-3.70 (m, 4H, CH and OCH_3), 3.92 (s, 3H, OCH_3), 4.83 (q, J = 7.2 Hz, 1H, αCH Phe), 6.18 (d, J = 6.8 Hz, 1H, NH Phe), 6.67 (q, J = 7.2 Hz, 1H, βCH ΔAbu), 7.04-7.17 (m, 8H, H Ar and NH ΔAbu), 7.25 (dd, J = 2.0 Hz, 1H, Ar H), 7.56 (s, 1H, Ar H), 7.64 (dd, J = 8.4 and 8.8 Hz, 2H, Ar H); ^{13}C NMR (100.6 MHz, $CDCl_3$, δ): 14.15 (γCH_3 ΔAbu), 18.08 (CH_3), 37.19 (βCH_2 Phe), 46.76 (CH), 52.11 (OCH_3), 54.27 (αCH Phe), 55.27 (OCH_3), 105.53 (CH), 119.06 (CH), 125.85 (C), 126.01 (CH), 126.06 (CH), 126.81 (CH), 127.52 (CH), 128.47 (CH), 128.90 (C), 129.17 (CH), 129.24 (CH), 133.75 (C), 134.28 (CH), 135.32 (C), 136.18 (C), 157.72 (C-O), 164.39 (C=O), 169.36 (C=O), 174.91 (C=O); HRMS (micrOTOF) *m/z*: $[M + Na]^+$ calcd for $C_{28}H_{30}N_2NaO_5$ 497.20524; found, 497.20604.

*Synthesis of Npx-L-Val-Z-ΔPhe-OMe (**4c**):* The general procedure described above was followed with compound **3c** (0.59 g, 1.5 mmol) giving compound **4c** (0.50 g, 68 %) as a white solid; mp 213.0-214.0 ºC; ^{1}H NMR (400 MHz, DMSO-d_6, δ): 0.91 (d, J = 6.8 Hz, 3H, γCH_3 Val), 0.96 (d, J = 6.4 Hz, 3H, γCH_3 Val), 1.43 (d, J = 7.2 Hz, 3H, CH_3), 1.97-2.07 (m, 1H, βCH Val), 3.60 (s, 3H, OCH_3), 3.83 (s, 3H, OCH_3), 3.96 (q,

View Article Online
DOI: 10.1039/C5TB00501A
Journal Name

J = 6.8 Hz, 1H, CH), 4.82 (t, *J* = 8.0 Hz, 1H, *α*CH Val), 7.04-7.11 (m, 4H, Ar H), 7.18 (s, 1H, *β*CH ΔPhe), 7.24 (d, *J* = 2.4 Hz, 1H, Ar H), 7.47 (dd, *J* = 2.0 and 8.8 Hz, 1H, Ar H), 7.51 (dd, *J* = 2.0 and 8.4 Hz, 2H, Ar H), 7.66 (d, *J* = 4.8 Hz, 1H, Ar H), 7.69 (d, *J* = 4.4 Hz, 1H, Ar H), 7.72 (s, 1H, Ar H), 8.14 (d, *J* = 8.8 Hz, 1H, NH Val), 9.73 (brs, 1H, NH ΔPhe); ^{13}C NMR (100.6 MHz, DMSO-d_6, δ): 18.34 (*γ*CH_3 Val), 19.17 (*γ*CH_3 Val), 19.34 (CH_3), 30.64 (*β*CH Val), 40.13 (*α*CH Val), 52.05 (OCH_3), 55.19 (OCH_3), 57.70 (CH), 105.72 (CH), 118.49 (CH), 125.42 (CH), 125.85 (C), 126.50 (CH), 126.73 (CH), 128.41 (C), 128.45 (CH), 129.10 (CH), 129.27 (CH), 129.98 (CH), 132.37 (CH), 133.08 (C), 133.17 (C), 137.38 (C), 156.99 (C-O), 165.32 (C=O), 171.37 (C=O), 173.76 (C=O); HRMS (micrOTOF) *m/z*: [M + Na]$^+$ calcd for $C_{29}H_{32}N_2NaO_5$ 511.22089; found, 511.22136.

*Synthesis of Npx-L-Ala-Z-ΔPhe-OMe (**4d**):* The general procedure described above was followed with compound **3d** (0.70 g, 2 mmol) giving compound **4d** (0.62 g, 67 %) as a white solid; mp 169.0-170.0 ºC; ^{1}H NMR (400 MHz, $CDCl_3$, δ): 1.37 (d, *J* = 7.2 Hz, 3H, *β*CH_3 Ala), 1.55 (d, *J* = 7.2 Hz, 3H, CH_3), 3.70 (s, 4H, CH and OCH_3), 3.90 (s, 3H, OCH_3), 4.68-4.76 (m, 1H, *α*CH Ala), 6.29 (d, *J* = 6.4 Hz, 1H, NH Ala), 7.05 (d, *J* = 2.4 Hz, 1H, Ar H), 7.09-7.12 (dd, *J* = 2.4 and 6.4 Hz, 1H, Ar H), 7.22-7.24 (m, 3H, Ar H), 7.26-7.29 (dd, *J* = 1.6 and 6.8 Hz, 1H, Ar H), 7.33 (s, 1H, *β*CH ΔPhe), 7.38-7.40 (m, 2H, Ar H), 7.60 (s, 2H, Ar H), 7.62 (s, 1H, Ar H), 8.02 (brs, 1H, NH ΔPhe); ^{13}C NMR (100.6 MHz, $CDCl_3$, δ): 17.58 (*β*CH_3 Ala), 18.37 (CH_3), 46.73 (CH), 49.11 (*α*CH Ala), 52.48 (OCH_3), 55.27 (OCH_3), 105.57 (CH), 119.05 (CH), 123.66 (*α*C), 125.94 (CH), 126.09 (CH), 127.57 (CH), 128.46 (CH), 128.91 (C), 129.21 (CH), 129.47 (CH), 129.69 (CH), 133.73 (*β*CH ΔPhe), 133.33 (C), 133.73 (C), 135.64 (C), 157.68 (C-O), 165.21 (C=O), 171.00 (C=O), 174.76 (C=O); HRMS (ESI) *m/z*: [M + Na]$^+$ calcd for $C_{27}H_{28}N_2NaO_5$ 483.18904; found, 483.18917.

*Synthesis of Npx-L-Ala-Z-ΔAbu-OMe (**4e**):* The general procedure described above was followed with compound **3e** (0.69 g, 2.4 mmol) giving compound **4e** (0.89 g, 92 %) as a white solid; mp 150.0-151.0 ºC; ^{1}H NMR (300 MHz, $CDCl_3$, δ): 1.38 (d, *J* = 7.2 Hz, 3H, *β*CH_3 Ala), 1.50 (d, *J* = 7.5 Hz, 3H, *γ*CH_3 ΔAbu), 1.58 (d, *J* = 7.2 Hz, 3H, CH_3), 3.63 (s, 3H, OCH_3), 3.73 (q, *J* = 7.2 Hz, 1H, CH), 3.89 (s, 3H, OCH_3), 4.66-4.76 (m, 1H, *α*CH Ala), 6.49 (d, *J* = 7.5 Hz, 1H, NH Ala), 6.66 (q, *J* = 7.2 Hz, 1H, *β*CH ΔAbu), 7.06 (d, *J* = 2.4 Hz, 1H, Ar H), 7.09-7.13 (dd, *J* = 2.7 and 6.3 Hz, 1H, Ar H), 7.31-7.35 (dd, *J* = 1.5 and 6.9 Hz, 1H, Ar H), 7.62-7.66 (m, 3H, Ar H), 7.91 (brs, 1H, NH ΔAbu); ^{13}C NMR (75.4 MHz, $CDCl_3$, δ): 13.92 (*γ*CH_3 ΔAbu), 17.86 (*β*CH_3 Ala), 18.27 (CH_3), 46.61 (CH), 48.86 (*α*CH Ala), 52.08 (OCH_3), 55.22 (OCH_3), 105.48 (CH), 118.97 (CH), 125.98 (CH and *α*C), 126.44 (C), 127.40 (CH), 128.85 (CH), 129.17 (CH), 133.67 (C), 134.50 (*β*CH ΔAbu), 135.66 (C), 157.60 (C-O), 164.45 (C=O), 170.83 (C=O), 174.68 (C=O); Anal. calcd for $C_{22}H_{26}N_2O_5$: C 66.32, H 6.58, N 7.03; found: C 66.23, H 6.25, N 6.51.

*Synthesis of dehydrodipeptides **5a-e**:* NaOH (1 equiv, 1 M) was added to a solution of *N*-acyl dehydrodipeptide methyl ester (**4a-e**) in dioxane (3 mL). The solution was stirred at room temperature (the reaction was followed by TLC until no starting material was detected). The dioxane was removed under reduced pressure and the reaction mixture was acidified to pH 2–3 with HCl (1 M) and the solid formed filtered.

*Synthesis of Npx-L-Phe-Z-ΔPhe-OH (**5a**):* The general procedure described above was followed with compound **4a** (0.268 g, 0.5 mmol) giving compound **5a** (0.183 g, 70 %) as a white solid; mp 195.0-196.0 ºC; ^{1}H NMR (400 MHz, DMSO-d_6, δ): 1.21 (d, *J* = 7.2 Hz, 3H, CH_3), 2.80-2.86 (dd, *J* = 10.8 and 13.6 Hz, 1H, *β*CH_2 Phe), 3.11-3.15 (dd, *J* = 3.6 and 14.0 Hz, 1H, *β*CH_2 Phe), 3.76 (q, *J* = 7.2 Hz, 1H, CH), 3.83 (s, 3H, OCH_3), 4.72-4.78 (m, 1H, *α*CH Phe), 7.09 (dd, *J* = 2.4 and 8.8 Hz, 1H, Ar H), 7.17-7.28 (m, 8H, Ar H), 7.31-7.33 (m, 2H, Ar H), 7.37 (dd, *J* = 1.6 and 8.4 Hz, 1H, Ar H), 7.51-7.74 (m, 2H, Ar H), 7.65-7.68 (m, 3H, □-CH + Ar H), 8.31 (d, *J* = 8.8 Hz, 1H, NH Phe), 9.68 (s, 1H, NH ΔPhe), 12.71 (brs, 1H, CO_2H); ^{13}C NMR (100.6 MHz, DMSO-d_6, δ): 18.86 (CH_3), 37.33 (*β*CH_2 Phe), 44.64 (CH), 53.80 (*α*CH Phe), 55.10 (OCH_3), 105.62 (CH), 118.37 (CH), 125.34 (CH), 126.23 (CH), 126.35 (C), 126.39 (CH), 126.65 (CH), 127.99 (CH), 128.29 (C), 128.36 (CH), 128.45 (CH), 129.04 (CH), 129.32 (CH), 129.91 (CH), 131.83 (CH), 133.04 (C), 133.50 (C), 137.07 (C), 137.87 (C), 156.89 (C-O), 166.14 (C=O), 170.93 (C=O), 173.33 (C=O); HRMS (ESI) *m/z*: [M + Na]$^+$ calcd for $C_{32}H_{30}N_2NaO_5$ 545.20469; found, 545.20483.

*Synthesis of Npx-L-Phe-Z-ΔAbu-OH (**5b**):* The general procedure described above was followed with compound **4b** (0.17 g, 0.36 mmol) giving compound **5b** (0.160 g, 97 %) as a white solid; mp 186.0-187.0 ºC; ^{1}H NMR (400 MHz, DMSO-d_6, δ): 1.21 (d, *J* = 7.2 Hz, 3H, CH_3), 1.47 (d, *J* = 7.2 Hz, 3H, *γ*CH_3 ΔAbu), 2.80-2.86 (dd, *J* = 10.0 and 3.6 Hz, 1H, *β*CH_2 Phe), 3.06-3.11 (dd, *J* = 4.4 and 9.2 Hz, 1H, *β*CH_2 Phe), 3.77 (q, *J* = 6.8 Hz, 1H, CH), 3.84 (m, 3H, OCH_3), 4.68-4.74 (m, 1H, *α*CH Phe), 6.50 (q, *J* = 7.2 Hz, 1H, *β*CH ΔAbu), 7.11 (dd, *J* = 2.8 and 6.0 Hz, 1H, Ar H), 7.18-7.31 (m, 6H, Ar H), 7.56 (s, 1H, Ar H), 7.37 (dd, *J* = 1.6 and 6.8 Hz, 1H, Ar H) 7.64-7.73 (m, 2H, Ar H), 8.28 (d, *J* = 8.4 Hz, 1H, NH Phe), 9.19 (s, 1 H, NH ΔAbu), 12.48 (brs, 1H, CO_2H); ^{13}C NMR (100.6 MHz, DMSO-d_6, δ): 13.52 (*γ*CH_3 ΔAbu), 18.55 (CH_3), 37.90 (*β*CH_2 Phe), 44.57 (CH), 53.64 (*α*CH Phe), 55.10 (OCH_3), 105.62 (CH), 118.42 (CH), 125.29 (CH), 126.21 (CH), 126.60 (CH), 127.93 (CH), 127.98 (C), 128.30 (C), 129.04 (CH), 129.16 (CH), 129.32 (CH), 132.11 (CH), 133.05 (C), 137.02 (C), 137.79 (C), 156.91 (C-O), 165.37 (C=O), 169.88 (C=O), 173.17 (C=O); HRMS (ESI) *m/z*: [M + Na]$^+$ calcd for $C_{27}H_{28}N_2NaO_5$ 483.18904; found, 483.18921.

*Synthesis of Npx-L-Val-Z-ΔPhe-OH (**5c**):* The general procedure described above was followed with compound **4c** (0.43 g, 0.88 mmol) giving compound **5c** (0.35 g, 85 %) as a white solid; mp 218.0-219.0 ºC; ^{1}H NMR (400 MHz, DMSO-d_6, δ): 0.90 (d, *J* = 6.4 Hz, 3H, *γ*CH_3 Val), 0.96 (d, *J* = 6.4 Hz, 3H, *γ*CH_3 Val), 1.43 (d, *J* = 7.2 Hz, 3H, CH_3), 2.00-2.09 (m, 1H, *β*CH Val), 3.84 (s, 3H, OCH_3), 3.96 (q, *J* = 7.2 Hz, 1H, CH), 4.36 (t, *J* = 8.0 Hz, 1H, *α*CH Val), 6.99-7.11 (m, 4H, Ar H), 7.20 (s, 1H, *β*CH ΔPhe), 7.24 (d, *J* = 2.8 Hz, 1H, Ar H), 7.45-7.52 (m, 3H, Ar H), 7.67-7.72 (dd, *J* = 2.4 and 6.4 Hz, 2H,

Journal Name

View Article Online
DOI: 10.1039/C5TB00501A ARTICLE

Ar H), 7.72 (s, 1H, Ar H), 8.11 (d, J = 9.2 Hz, 1H, NH Val), 9.54 (s, 1H, NH ΔPhe), 12.67 (brs, 1H, CO_2H); ^{13}C NMR (100.6 MHz, DMSO-d_6, δ): 18.27 (γCH_3 Val), 19.23 (γCH_3 Val), 19.32 (CH_3), 30.66 (βCH Val), 44.45 (CH), 55.11 (OCH_3), 57.62 (αCH Val), 105.64 (CH), 118.39 (CH), 125.35 (CH), 126.41 (CH), 126.67 (C), 126.69 (CH), 128.24 (CH), 128.35 (C), 128.82 (CH), 129.05 (CH), 129.76 (CH), 131.81 (CH), 133.08 (C), 133.45 (C), 137.34 (C), 156.90 (C-O), 166.13 (C=O), 170.91 (C=O), 173.59 (C=O); HRMS (ESI) *m/z*: $[M + Na]^+$ calcd for $C_{28}H_{30}N_2NaO_5$ 497.20469; found, 497.20479.

*Synthesis of Npx-L-Ala-Z-ΔPhe-OH (**5d**):* The general procedure described above was followed with compound **4d** (0.46 g, 1 mmol) giving compound **5d** (0.38 g, 85 %) as a white solid; mp 185.0-186.0 ºC; ^1H NMR (400 MHz, DMSO-d_6, δ): 1.30 (d, J = 6.8 Hz, 3H, βCH_3 Ala), 1.41 (d, J = 6.4 Hz, 3H, CH_3), 3.83-3.86 (m, 4H, OCH_3 and CH), 4.44-4.52 (m, 1H, αCH Ala), 7.08-7.11 (dd, J = 2.4 and 6.4 Hz, 1H, Ar H), 7.19-7.23 (m, 5H, Ar H), 7.43-7.46 (dd, J = 1.6 and 6.8 Hz, 1H, Ar H), 7.52-7.55 (m, 2H, βCH ΔPhe and Ar H), 7.66-7.71 (m, 3H, Ar H), 8.23 (d, J = 7.6 Hz, 1H, NH Ala), 9.43 (s, 1H, NH ΔPhe), 12.64 (brs, 1H, CO_2H); ^{13}C NMR (100.6 MHz, DMSO-d_6, δ): 17.95 (βCH_3 Ala), 18.85 (CH_3), 44.41 (CH), 48.11 (αCH Ala), 55.10 (OCH_3), 105.63 (CH), 118.38 (CH), 125.34 (CH), 126.28 (C), 126.43 (CH), 126.62 (CH), 128.32 (CH), 129.02 (C), 129.04 (CH), 129.05 (CH), 129.87 (CH), 131.87 (CH), 133.04 (C), 133.49 (C), 137.24 (C), 156.89 (C-O), 166.11 (C=O), 171.78 (C=O), 173.18 (C=O); HRMS (ESI) *m/z*: $[M + Na]^+$ calcd for $C_{26}H_{26}N_2NaO_5$ 469.17339; found, 469.17353.

*Synthesis of Npx-L-Ala-Z-ΔAbu-OH (**5e**):* The general procedure described above was followed with compound **4e** (0.40 g, 1 mmol) giving compound **5e** (0.31 g, 80 %) as a white solid; mp 170.0-171.0 ºC; ^1H NMR (400 MHz, DMSO-d_6, δ): 1.27 (d, J = 7.2 Hz, 3H, βCH_3 Ala), 1.39 (d, J = 7.2 Hz, 3H, CH_3), 1.47 (d, J = 7.2 Hz, 3H, γCH_3 ΔAbu), 3.84-3.86 (m, 4H, OCH_3 and CH), 4.40-4.47 (m, 1H, αCH Ala), 6.47 (q, J = 7.2 Hz, 1H, βCH ΔAbu), 7.09-7.13 (dd, J = 2.4 and 6.4 Hz, 1H, Ar H), 7.24 (d, J = 2.4 Hz, 1H, Ar H), 7.42-7.45 (dd, J = 2.0 and 6.8 Hz, 1H, Ar H), 7.68-7.74 (m, 3H, H Ar), 8.21 (d, J = 7.6 Hz, 1H, NH Ala), 8.94 (s, 1H, NH ΔAbu), 12.41 (brs, 1H, CO_2H); ^{13}C NMR (100.6 MHz, DMSO-d_6, δ): 13.46 (γCH_3 ΔAbu), 18.45 (CH_3), 18.53 (CH_3), 44.39 (CH), 48.05 (αCH Ala), 55.10 (OCH_3), 105.64 (CH), 118.44 (CH), 125.29 (CH), 126.45 (CH), 126.59 (CH), 127.94 (αC), 128.33 (C), 129.04 (CH), 132.05 (CH), 133.06 (C), 137.18 (C), 156.91 (C-O), 165.33 (C=O), 170.88 (C=O), 173.09 (C=O); HRMS (ESI) *m/z*: $[M + Na]^+$ calcd for $C_{21}H_{24}N_2NaO_5$ 407.15774; found, 407.15778.

Conclusions

Several *N*-aromatic dehydrodipeptide amphiphiles were prepared and studied as new hydrogelators. Molecular dynamic simulations were used to obtain insights into the underlying molecular mechanism responsible for aggregation. The results obtained were in excellent agreement with the experimental observations. This allowed the rationalization of the structural features that govern the self-assembly of dehydrodipeptide amphiphiles. Thus compounds with at least one aromatic amino acid give hydrogels in low critical gelation concentrations. TEM images of the new hydrogels prepared revealed that they comprise nanofibers with different widths that entangle to give a 3D network. All hydrogels showed a viscoelastic behaviour with a storage modulus higher than the loss modulus and independent from the frequency. The CD spectra of two hydrogelators, **5a** and **5b**, were compared with that obtained from the dipeptide phenylalanylphenylalanine *N*-protected with naproxen. The CD spectra were similar and point to a structural organization with the characteristics of a β-sheet arrangement. Fluorescence spectroscopy studies showed that this is a good methodology to determine the CGC and the gelation pH. Preliminary toxicity assays were performed using one of the hydrogelators and it was found that this compound was not toxic even at concentrations of 500 μM. The resistance of some of the new hydrogelators towards α-chymotrypsin was tested in an 80 h assay and it was found that the presence of the dehydroamino acid in the conjugates confers proteolytic resistance to the hydrogelator. Giving the properties of this new class of hydrogelators it is possible to conclude that they constitute promising candidates for biomedical applications.

Acknowledgements

Thanks are due to Foundation for Science and Technology (FCT) – Portugal, QREN and program FEDER/COMPETE for financial support through Centre of Chemistry (CQ-UM) of University of Minho. FCT is also acknowledged for PhD grants of G. Pereira (SFRH/BD/38766/2007), H. Vilaça (SFRH/BD/72651/2010) and T. G. Castro (SFRH/BD/79195/2011), co-funded by the European Social Fund. The NMR spectrometer Bruker Avance III 400 is part of the Portuguese NMR Network (Rede/1517/RMN/2005) which is also supported by the FCT.

Notes and references

[a] Department of Chemistry
University of Minho
Campus de Gualtar, 4710-057 Braga, Portugal
E-mail: pmf@quimica.uminho.pt .
[b] Department of Physics
University of Minho
Campus de Gualtar, 4710-057 Braga, Portugal.
[c] Centre for Neuroscience and Cell Biology
University of Coimbra
Coimbra 3004-517, Portugal
[c] Department of Chemistry
Brandeis University
Waltham, MA, 02454 USA.

View Article Online
DOI: 10.1039/C5TB00501A
Journal Name

1 J. Kopecek, J. Yang, *Angew. Chem. Int. Ed.* 2012, **51**, 7396.
2 S. Marchesan, Y. Qu, L. J. Waddington, C. D. Easton, V. Glattauer, T. J. Lithgow, K. M. McLean, J. S. Forsythe, P. G. Hartley, *Biomaterials* 2013, **34**, 3678.
3 M. Guvendiren, H. D. Lu, J. A. Burdick, *Soft Matter* 2012, **8**, 260.
4 G. Fichman, E. Gazit, *Acta Biomaterialia* 2014, **10**, 1671.
5 A. Raspa, G.A.A. Saracino, R. Pugliese, D. Silva, D. Cigognini, A. Vescovi, F. Gelain *Adv. Funct. Mater.* 2014, **24**, 6317.
6 M. Ma, Y. Kuang, Y. Gao, Y. Zhang, P. Gao, B. Xu, *J. Am. Chem. Soc.* 2010, **132**, 2719.
7 B. Frohm, J.E. DeNizio, D.S.M. Lee, L. Gentile, U. Olsson, J. Malm, K. S. Akerfeldt, S. Linse, *Soft Matter*, 2015, **11**, 414.
8 C. Tang, R. V. Ulijn, A. Saiani, *Langmuir* 2011, *27*, 14438.
9 Z.Yang, G. Liang, Ma. Ma, Y. Gao, B. Xu, *Small* 2007, **3**, 558.
10 G. Liang, Z. Yang, R. Zhang, L. Li, Y. Fan, Y. Kuang, Y. Gao, T. Wang, W.W. Lu, B. Xu, *Langmuir*, 2009, **25**, 8419.
11 X. Li, X. Du, J. Li, Y. Gao, Y. Pan , J. Shi, N. Zhou, B. Xu, *Langmuir*, 2012, **28**, 13512.
12 J.Li, Y. Gao, Yi Kuang, J. Shi, X. Du, J. Zhou, H. Wang, Z. Yang, B. Xu, *J. Am. Chem. Soc.*, 2013, **135**, 9907.
13 M. M. Nguyen, K. M. Eckes, L. J. Suggs, *Soft Matter* 2014, ***10***, 2693.
14 J. Li, Y. Kuang, Y. Gao , X. Du, J. Shi, B. Xu, *J. Am. Chem. Soc.* 2013, **135**, 542.
15 J. Li, Y. Kuang, J. Shi, Y. Gao, J. Zhou, B. Xu, *Beilstein J. Org. Chem.* 2013, **9**, 908.
16 P. M. T. Ferreira, H. L. S. Maia, L. S. Monteiro, J. Sacramento, *J. Chem. Soc., Perkin Trans. 1* 1999, 3697.
17 P. M. T. Ferreira, L. S. Monteiro, G. Pereira, L. Ribeiro, J. Sacramento, L. Silva, *Eur. J. Org. Chem.* 2007, 5934.
18 A. S. Abreu, P. M. T. Ferreira, L. S. Monteiro, M. J. R. P. Queiroz, I. C. F. R. Ferreira, R. C. Calhelha, L. M. Estevinho, *Tetrahedron* 2004, ***60***, 11821.
19 P. M. T. Ferreira, E. M. S. Castanheira, L. S. Monteiro, G. Pereira, H. Vilaça, *Tetrahedron* 2010, **66**, 8672.
20 P. M. T. Ferreira, L. S. Monteiro, G. Pereira, E. M. S. Castanheira, C. G. Frost, *Eur. J. Org. Chem*. 2013, **3**, 550.
21 G. Pereira, H. Vilaça, P. M. T. Ferreira, *Amino Acids* 2013, **44**, 335.
22 a) G. Laverty, A. P. McCloskey, B. F. Gilmore, D. S. Jones, J. Zhou, B. Xu, *Biomacromolecules* 2014, **15**, 3429; b) Y. Gao, Y. Kuang, X. Du, J. Zhou, P. Chandran, F. Horkay, B. Xu, *Langmuir* 2013, **29**, 15191; c) J. Raeburn. T. O. McDonald, D. J. Adams, *Chem. Commun.* 2012, **48**, 9355; d) X. Li, X. Du, J. Li, Y. Gao, Y. Pan, J. Shi, N. Zhou, B. Xu, *Langmuir* 2012, **28**, 13512; e) L. Chen, G. Pont, K. Morris, G. Lotze, A. Squires, L. C. Serpell, D. J. Adams, *Chem. Commun.* 2011, **47**, 12071; f) Y. Zhang, Y. Kuang, Y. Gao, B. Xu, *Langmuir* 2011, **27**, 529.
23 H. J. C. Berendsen, J. R. Grigera, T. P. Straatsma, *J. Phys. Chem.* 1987, **91**, 6269.
24 M. O. Sinnokrot, E. F. Valeev, C. D. Sherrill, *J. Am. Chem. Soc.* 2002**, 124**, 10887.
25 Schrödinger, *The PyMOL Molecular Graphics System*, 1.3r1; LLC: 2010.
26 M. M. Velazquez, M. Valero, L. J. Rodríguez, S. M. B. Costa, M. A. Santos, *J. Photochem. Photobiol. B: Biol.* 1995, **29**, 23.
27 G. D. Fasman, *Handbook of Biochemistry and Molecular Biology*, Proteins, I, 3rd Ed., CRC Press, 1976.
28 L. Chen, K. Morris, A. Laybourn, D. Elias, M. R. Hicks, A. Rodger, L. Serpell, D. J. Adams, *Langmuir* 2010, **26**, 5232.
29 N. Berova, L. D. Bari, G. Pescitelli, *Chem. Soc. Rev.* 2007, **36**, 914.
30 G. Impellizzeri, F. D´Alessandro, G. Pappalardo, C. Tringali, *J. Inc. Phenom.* 2005, **51**, 173.
31 K. Nakanishi, N. Berova, R. W. Woody, *Circular Dichroism Principles and Applications*, VCH Publishers Inc, New York 1994.
32 X. Li, K. Yi, J. Shi, Y. Gao, H.-C. Lin, B. Xu, *J. Am. Chem. Soc*. 2011, **133**, 17513.
33 S. Debnath, A. Shome, D.Das, P. K. Das, *J. Phys. Chem. B* 2010, **114**, 4407.
34 A. M. Smith, R. J. Williams, C. Tang, P. Coppo, R. F. Collins, M. L. Turner, A. Saiani, R. V. Ulijn, *Advanced Materials* 2008, **20**, 37.
35 H. F. Chow, J. Zhang, *Tetrahedron* 2005, **61**, 11279.
36 W. Huang, Z. X. Lin, W. F. van Gunsteren, *J. Chem. Theory Comput.* 2011**, 7**, 1237.
37 N. Schmid, A. P. Eichenberger, A. Choutko, S. Riniker, M. Winger, A. E. Mark, W. F. van Gunsteren, *Eur. Biophys. J. Biophys. Lett.* 2011**, 40**, 843.
38 B. Hess, C. Kutzner, D. van der Spoel, E. Lindahl, *J. Chem. Theory Comput.* 2008**, 4**, 435.
39 D. van der Spoel, E. Lindahl, B. Hess, A. R. Buuren, E. Apol, P. J. Meulenhoff, P. Tieleman, A. L. T. M. Sjibers, K. A. Feenstra, R. Drunen, H. J. C. Berendsen, *Gromacs user manual version 4.5*. 2010. www.gromacs.org
40 H. J. C. Berendsen, J. P. M. Postma, W. F. Vangunsteren, A. Dinola, J. R. Haak, *J. Chem. Phys*. 1984**, 81**, 3684.
41 D. van der Spoel, P. J. van Maaren, H. J. C. Berendsen, *J. Chem. Phys.* 1998**, 108**, 10220.
42 B. Hess, H. Bekker, H. J. C. Berendsen, J. Fraaije, *J. Comput. Chem.* 1997, **18**, 1463.
43 P. M. T. Ferreira, L. S. Monteiro, G. Pereira, *Amino Acids* 2010, **39**, 499.
44 A. S. Abreu, E. M. S. Castanheira, P. M. T. Ferreira, L. S. Monteiro, G. Pereira, M. J. R. P. Queiroz, *Eur. J. Org. Chem.* 2008, 5697.
45 R. Ramesh, K. De, S. Chandrasekaran, *Tetrahedron* 2007, **63**, 10534.